

## IMPROVED DIELECTRIC AND MAGNETIC PROPERTIES OF DILUTED MAGNETIC SEMICONDUCTOR $Zn_{1-x}Mn_xO$

Ehsan Uddin Ahmad<sup>1</sup>, M.K.R. Khan<sup>2</sup>, M. Bodiul Islam<sup>3,\*</sup>, M.A. Hadi Shah<sup>4</sup> and M. Mozibur Rahman<sup>5</sup>

<sup>1</sup>Department of Physics, Cambrian College, Campus-4, Dhaka-1229, Bangladesh

<sup>2,5</sup>Department of Physics, University of Rajshahi, Rajshahi-6205, Bangladesh

<sup>3</sup>Department of Glass and Ceramic Engineering (GCE), Rajshahi University of Engineering & Technology (RUET), Rajshahi-6204, Bangladesh

<sup>4</sup>Department of Physics, Rajshahi University of Engineering & Technology (RUET), Rajshahi-6204, Bangladesh

<sup>1</sup>ehsanrubd@gmail.com, <sup>2</sup>fkrkhan@yahoo.co.uk, <sup>3,\*</sup>mbislam\_mst@yahoo.com, <sup>4</sup>mahsphys@gmail.com, <sup>5</sup>mozibur2000@yahoo.com

**Abstract-** Manganese doped ZnO samples,  $Zn_{1-x}Mn_xO$  ( $x = 0 \leq x \leq 0.09$ ), have synthesized by solid-state reaction method and studied their structural, dielectric and magnetic properties. XRD study suggests that the solubility limit of Mn in ZnO is  $x < 0.07$ . A tiny phase segregation of  $MnO_2$  and  $Mn_2O_3$  is observed beyond ~7% of Mn doping in ZnO. The room temperature resistance of Mn-doped samples is about 20 times higher than undoped ZnO. The activation energy of the synthesized samples estimated at high temperature region lies between 1.17 – 1.30 eV which is almost independent of Mn/Zn ratio. The real part of dielectric constant changes with Mn/Zn ratio. The magnitude is comparatively high at lower frequency region and becomes constant at frequency  $\geq 20$  KHz. The magnetization  $M$  was measured as a function of the applied magnetic field  $H$  at room temperature and the magnetic properties depend on the Mn concentration.

**Keywords:** Diluted magnetic semiconductor, Solid-state reaction, XRD, IR

### 1. INTRODUCTION

Diluted magnetic semiconductors (DMS) are subjects of intense interest because of the prospect of their application in the emerging field of spintronics [1]. ZnO is a wide band gap (3.37 eV) semiconductor with a large exciton binding energy (60 meV) and is one of the promising candidates for making a DMS by doping with a magnetic element [2, 3]. Theoretical predictions of room temperature ferromagnetism in ZnO based DMS have caused intensive efforts on ZnO material doped with transition metal [4]. The Mn-doped ZnO system is very promising due to its wide bandgap of ZnO host material and due to its high solubility of Mn atoms in ZnO matrix. Magnetic semiconductors are materials that exhibit both ferromagnetism (and a similar response) and useful semiconductor properties. If implemented in devices, these materials could provide a new type of control of conduction. Whereas traditional electronics are based on control of charge carriers (n- or p-type), practical magnetic semiconductors would also allow control of quantum spin state (up and down). This would theoretically provide near-total spin polarization (as opposed to iron and other metals, which provide only ~50% polarization), which is an important property for spintronics applications, e.g. spin transistors. While many traditional magnetic materials, such as magnetite, are also semiconductors, materials scientists generally

predict that magnetic semiconductors will only find widespread use if they are similar to well-developed semiconductor materials. To that end, dilute magnetic semiconductors have recently been a major focus of magnetic semiconductor research. These are based on traditional semiconductors, but are doped with transition metal instead of, or in addition, electronically active elements. The aim of the present work is to prepare  $Zn_{1-x}Mn_xO$  ( $x = 0 \leq x \leq 0.09$ ) by solid-state reaction method. In this work, we have studied their structural, electrical, dielectric and magnetic properties.

### 2. SAMPLE PREPARATION AND EXPERIMENTAL SETUP

There are several methods that are commonly used for sample preparation which are mainly classified into four categories; (a) solid-state reaction method, (b) solution method, (c) melt quenched or glass ceramic method and (d) thin film method. For preparation of bulk sample, solid-state reaction method is used. So in this study, we used solid state reaction method for preparing Mn doped ZnO samples. Equipments used for preparing bulk samples by solid-state reaction method are balance, mortar and pestle, crucibles, furnace, pressure gauge, dice, ceramic plate, etc. In this method appropriate amount of the constituents are ground together and mixed thoroughly in a mortar. Ground powders are then

calcined in air or ambient atmosphere at 450 °C for 12 hours. The samples are then reground and reheated for several times to obtain the correct crystalline phase. The calcined chunk are then ground again to become fine powders and pressed in the form of pellets. These pellets are then sintered at 950 °C (not far below the melting point of the constituents) in air ambient atmosphere to obtain a single phase sample.

## 2.1 Grinding, mixing and calcining

At first, appropriate amounts of the mother material (ZnO, purity 99.7%, MERCK, India) and the dopant (MnO<sub>2</sub>, purity 99.9%, MERCK, Germany) samples were weighted out separately and kept in a ceramic mortar. Using a pestle these samples were grounded about 2 hours for proper mixing. The powder thus obtained was scrapped from the wall of the mortar and placed in an alumina crucible. Before placing the powder into the crucible, it was washed using distilled water and then with ethanol. The crucible which contained the grounded powder was then placed in the furnace and heated at 450 °C for 12 hours. Then the furnace temperature was set at the room temperature and allowed to furnace cool. When the furnace temperature was cooled down to room temperature, the sample was taken out and ground until it became fine powders. The same procedure was repeated for two times to obtain fine powders. Finally calcinations at 500 °C for 12 hours were carried out.

## 2.2 Pellet formation and sintering

About 1 gm of the powder was then put into a dice and pressed into pellets of about 13 mm diameter and 1-2 mm thick under a force of 20 KN held for about 10 minutes using a hydraulic pressure unit. The prepared pellets were then placed in a ceramic boat and this was inserted into a furnace for sintering at 950 °C for 12 hours. The sintering was done to obtain a crystalline phase of the material. The inherent color of ZnO is white. The colors of Zn<sub>0.99</sub>Mn<sub>0.01</sub>O, Zn<sub>0.98</sub>Mn<sub>0.02</sub>O, Zn<sub>0.97</sub>Mn<sub>0.03</sub>O, Zn<sub>0.95</sub>Mn<sub>0.05</sub>O, Zn<sub>0.93</sub>Mn<sub>0.07</sub>O and Zn<sub>0.91</sub>Mn<sub>0.09</sub>O were light yellow, yellow, deep yellow, tan, ash and black respectively.

## 2.3 Experimental setup for characterization

X-ray diffraction patterns of the powder samples were taken by using an X-ray diffractometer (X'pert pro PW 3040, Phillips) located at the Department of Electrical and Electronic Engineering, Toyohashi University of Technology, Japan, to check the homogeneity and possible phases of the specimens. The diffraction pattern collected for 2θ values in the scanning range (20-70) degree for all samples at a step sampling of 0.02 degree.

For electrical characterization, we have used the two-probe method (arrangements). In two-probe method, two connecting wires are connected (ohmic contact) by silver paste on the two opposite surfaces of the sample. The sample was positioned on a mica sheet placed on a heater. From the two junctions both current and voltage are measured. A small current in the range of microampere (μA) is passed through the sample and the voltage i.e. e.m.f. across the sample is monitored by a voltmeter (Keithley 614 electrometer, U.S.A.) as a

function of temperature at constant supply voltage. Circuit arrangement is shown in Fig. 1.

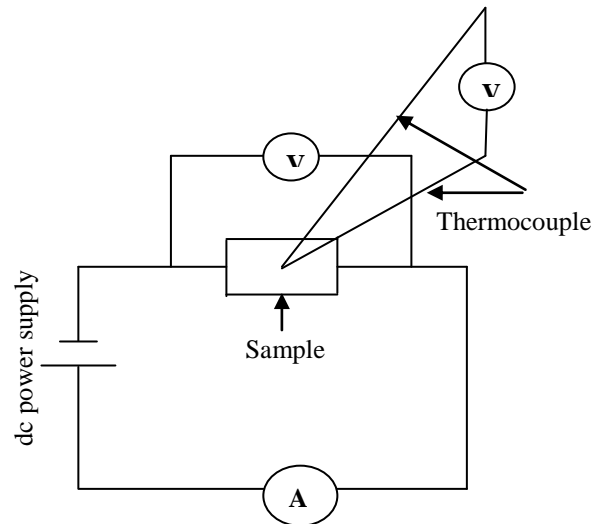


Fig.1: Circuit arrangement for resistance measurement

For the measurement of frequency dependent dielectric constant of the prepared samples we have used Precision Impedance Analyzer (Model 4294A, range 40 Hz-110 MHz, Agilent Technologies, Japan). The frequency dependent dielectric constants have taken in the frequency range of 40 Hz-100 KHz for all samples. The magnetization of the samples was measured by a Vibrating Sample Magnetometer (VSM).

## 3. RESULTS AND DISCUSSION

The results of various experimental measurements on zinc oxide (ZnO) and Mn doped zinc oxide (Mn:ZnO) bulk samples prepared by solid state reaction method have been presented in this section. Possible explanations and discussions of the results have also given.

### 3.1 Structural study

The X-ray diffraction (XRD) study has performed to check the crystallinity and phase of the samples. To get single phase and better quality, powder samples were calcined twice for 12 h at 450 °C followed by a final calcinations at 500°C for 12 h. This has been done so that constituent elements complete the chemical reaction, resulting homogeneous single phase compound. Calcined powder was then grind into fine powders and was used in XRD experiment. The crystallographic indexing of Miller planes from X-ray patterns of the samples were performed using standard JCPDS card.

The X-ray diffraction patterns for ZnO and Mn doped ZnO samples are shown in Fig. 2. The ZnO characteristic peaks are very sharp and no shoulder is found for other phases along with major crystallographic planes. The peaks were identified as (100), (002), (101), (102) and (110) comparing with the standard JCPDS card no 80-00075 (Grant Aid report in 1987). Three main ZnO peaks are found at around 31.80° (100), 34.52° (002) and 36.36° (100) in 2θ scale of Bragg angle. From X-ray patterns, it is also clear that as synthesized samples are crystalline and well oriented.

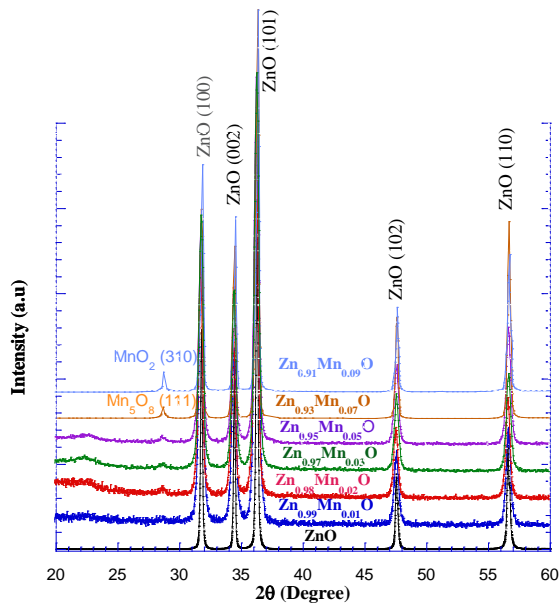


Fig.2: XRD patterns of  $Zn_{1-x}Mn_xO$  ( $x = 0 \geq x \geq 0.09$ ) samples

Fig. 2 clearly manifests that only the intense diffraction peak related to the wurtzite (hexagonal) ZnO upto  $x \leq 0.05$ . No diffraction peak of Mn or Manganese oxide phase segregation are found in the x-ray spectrum, but only a single-phased crystalline  $Zn_{1-x}Mn_xO$  is formed. It is noticed that the characteristics peak intensity is highest for undoped sample and with the doping of Mn, corresponding peak intensity decreased. With 1% (at wt.%) Mn doping, peak intensity is found to be lowest and the intensity increases gradually with increasing Mn concentrations shown in Fig. 3.

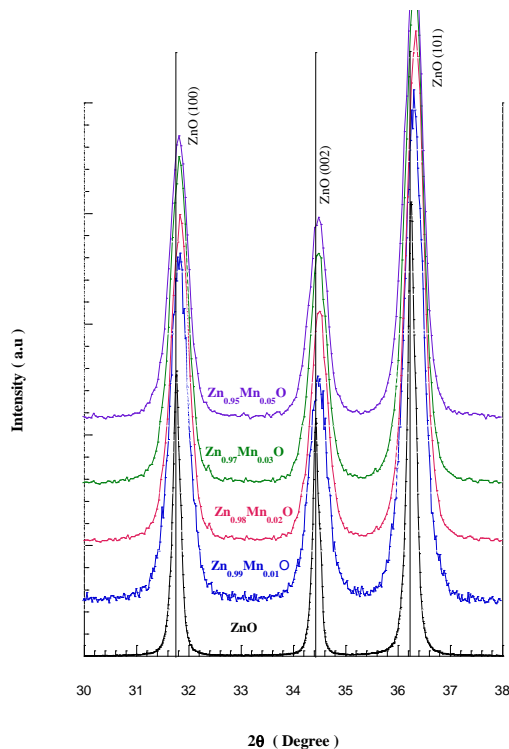


Fig.3: XRD patterns of (100), (002) and (101) peaks of  $Zn_{1-x}Mn_xO$  ( $x = 0 \geq x \geq 0.05$ ) samples

Fig. 2 also shows that there is an extra peak for the sample  $x \geq 0.07$  having very low intensity. The extra peak for  $x = 0.07$  sample at Bragg angle of  $28.71^\circ$  related to the Miller plane (111) and for  $x = 0.09$  sample the extra peak is at  $28.85^\circ$  and the corresponding Miller plane is (310). These two peaks do not match with ZnO that indicates the presence of impurity phases in the sample. Comparing Bragg angle and Miller plane of these two peaks to the standard JCPDS cards, (Card no. 39-1218 and 44-0141, PCPDFWIN v. 1.30) (1997), it is found that the above two peaks correspond to the monoclinic structure of  $Mn_5O_8$  and tetragonal structure of  $MnO_2$ . Analyzing, above experimental results the solubility of Mn in ZnO solid solution is estimated to be  $x \leq 0.05$ .

The lattice parameters and grain size of the samples calculated by Hess-Lipson method are tabulated in Table 1. From table, it is seen that both parameters  $a$  and  $c$  changes a very small with doping. R. D. Shannon [5] predicted that the lattice constants of  $Zn_{1-x}Mn_xO$  ( $x > 0$ ) ( $a = 3.2426 \text{ \AA}$  and  $c = 5.1907 \text{ \AA}$  for  $Zn_{0.98}Mn_{0.02}O$ ) were larger than those ( $a = 3.2403 \text{ \AA}$  and  $c = 5.1901 \text{ \AA}$ ) of pure ZnO, because the ionic radius of  $Mn^{2+}$  ( $0.66 \text{ \AA}$ ) is larger than that of  $Zn^{2+}$  ( $0.60 \text{ \AA}$ ). The expansion of the lattice constants of  $Zn_{1-x}Mn_xO$  also indicated that manganese was really doped into the ZnO structure. The full width at half maximum (FWHM) of the peaks (100), (002) and (101) are shown in Fig. 3 and the corresponding values of FWHM are 0.171, 0.160 and 0.184 degrees for  $x = 0$  samples. The FWHM value of Mn doped samples varies from 0.38 to 0.43 degrees. These small FWHM values suggest the high quality of the crystallites. For better clarity, extended view of diffraction patterns of (100), (002) and (101) peaks (30-38 degrees of  $2\theta$  scale) is shown in Fig. 3. A vertical line drawn through the middle of each of the peaks of ZnO profile (taking ZnO as a base material), it is clearly observed that the peak positions for increasing Mn concentration in bulk samples leads to the minor shift of the (100), (002) and (101) plane to the higher angle ( $2\theta$  scale) which indicates original ZnO lattice is being deformed due to the presence of Mn atoms. This experimental observation also proves the growth of  $Zn_{1-x}Mn_xO$  phase up to the solubility limit. Since the difference of ionic radii of Zn ( $0.60 \text{ \AA}$ ) and Mn ( $0.66 \text{ \AA}$ ) is very small, a very small change in lattice parameters are expected due to doping of Mn which corresponds to the experimental results given in Table 1.

Table 1: Lattice constants and  $c/a$  ratio of ZnO and Mn doped ZnO powders estimated from XRD study.

Mn in ZnO (%)	Lattice constants ( $\text{\AA}$ )		$c/a$ ratio
	$a$	$c$	
0	3.250	5.206	1.602
1	3.241	5.195	1.603
2	3.247	5.195	1.600
3	3.243	5.192	1.601
5	3.243	5.192	1.601
7	3.241	5.194	1.603
9	3.234	5.188	1.604

### 3.2 Electrical properties

Two probe arrangements were used to measure the resistance of the samples. The electrical resistances ( $R$ ) of the samples were calculated by using the relation  $R = V/I$ , where  $V$  is the applied voltage and  $I$  is the current that flows through the circuit. The room temperature (RT) resistance of ZnO is of the order of few  $K\Omega$  while the RT resistance of doped samples is very high of the order of few  $M\Omega$ . Fig. 4 shows the variation of electrical resistance with temperature for supply voltages  $V_s = 10$  volts. From this figure, it is clear that at room temperature, resistance is high but it decreases very sharply up to  $T \approx 370$  K and then decreases monotonically with temperature. The variation of resistance with temperature for ZnO sample is shown in the inset of Fig. 4.

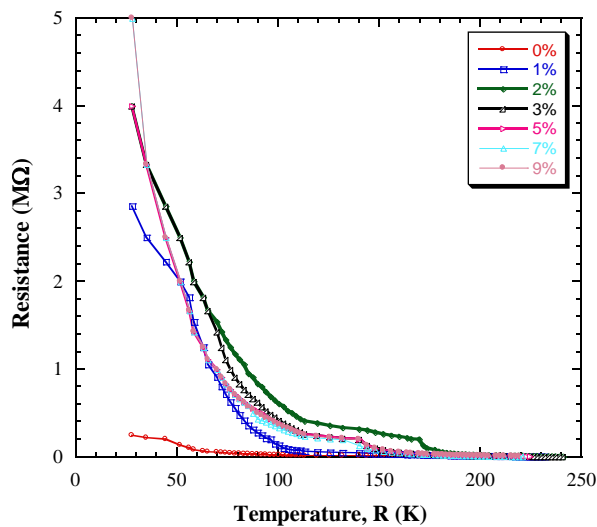


Fig.4: Variation of resistance with temperature for  $Zn_{1-x}Mn_xO$  ( $x = 0 \leq x \leq 0.09$ ) samples

It is also seen that the resistance of the Mn doped ZnO samples depends on mixing ratio of Mn in Zn. For pure ZnO, the resistance is comparatively low but with the increase of doping concentration of Mn into ZnO the resistance increased substantially. Mn is a group VII-A element. When Mn is mixed with ZnO, it may substitute Zn atom or may randomly distributed to grain boundaries during crystallization. Every Mn atom accepts one electron and as a result doping of Mn in ZnO attributes higher resistance of ZnO crystal.

Fig. 5 shows the variation of  $\ln R$  with  $T^{-1}$  for ZnO and Mn doped ZnO samples. The activation energy ( $\Delta E$ ) is calculated from these curves at temperature,  $T \geq 420$  K. The room temperature resistance and the calculated activation energy for different samples are tabulated in Table 2. From Table 2, it is seen that the activation energy for all samples at higher temperature ( $T \geq 420$  K) varies between 1.17 to 1.35 eV. The higher values of activation energies indicate the presence of deep level defect states. The resistance at higher temperature is low for ZnO and Mn doped ZnO and approximately constant, since at these temperature all the donor electrons have excited to conduction band.

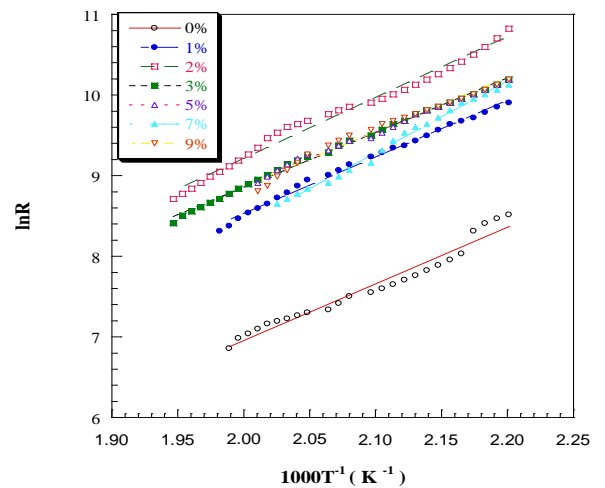


Fig.5: Plot for  $\ln R$  versus  $T^{-1}$  for undoped and Mn-doped ZnO samples

Table 2: Room temperature resistance ( $R_T$ ) and high temperature activation energy for different samples

Doping percentage (%)	Resistance $R_T$ ( $M\Omega$ )	Activation energy $E$ (eV)
0	0.24	1.20
1	2.9	1.21
2	4.0	1.30
3	4.0	1.30
5	4.0	1.17
7	5.0	1.35
9	5.0	1.20

### 3.3 Dielectric properties

The dielectric constant of the prepared samples was measured by precision impedance analyzer (Model 4294 A, Agilent Technologies, Japan). The dielectric constant ( $\epsilon$ ) was calculated by using the equation,  $\epsilon = Cd/\epsilon_0 A$ , where  $C$  is the capacitance of the sample at room temperature,  $\epsilon_0$  is the permittivity in the free space and  $A$  is the area of the sample.

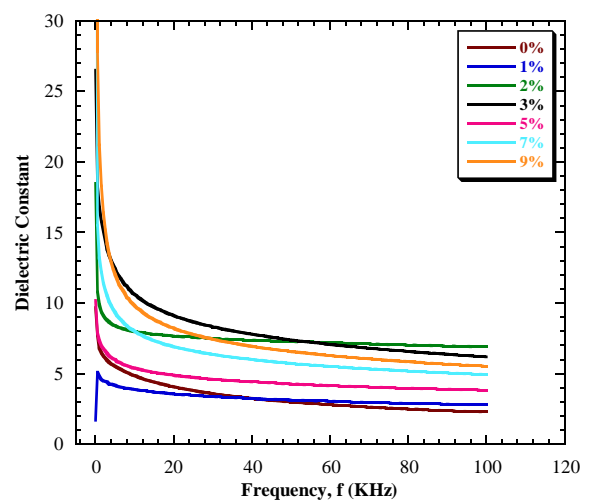


Fig.6: Variation of dielectric constant with frequency for ZnO and Mn doped ZnO samples in parallel circuit model.

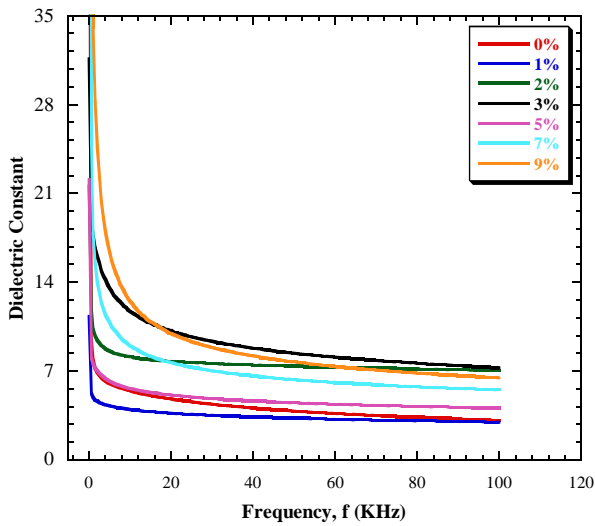


Fig.7: Variation of dielectric constant with frequency for ZnO and Mn doped ZnO samples in series circuit model

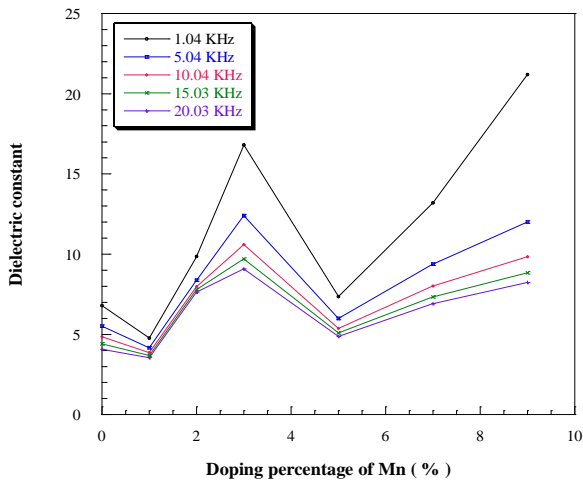


Fig.8: Variation of dielectric constant with doping of Mn into ZnO at different frequencies for parallel circuit

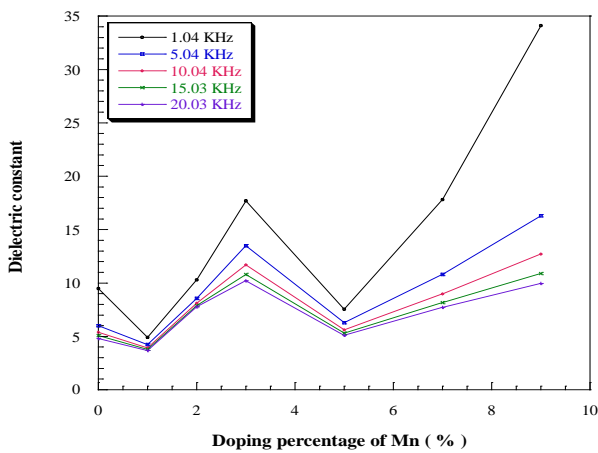


Fig.9: Variation of dielectric constant with doping of Mn into ZnO at different frequencies for series circuit

Figs. 6 and 7 show the variation of dielectric constant with frequency at room temperature for different samples in parallel and series circuit connections, respectively. It is seen from the figures that the dielectric constant for all samples is high at lower frequency region in comparison with higher frequency region. The dielectric constant remains almost constant after 20 KHz onwards for both parallel and series circuit connections.

Figs. 8 and 9 shows the variation of dielectric constant of Mn doped ZnO samples with different Mn/Zn ratios at different frequencies. The dielectric constant is found maximum for Mn = 9% at all frequencies.

### 3.4 Magnetic properties

Magnetization of the samples was determined with the help of Vibrating Sample Magnetometer (VSM). We have calibrated the VSM using a 152 mg spherical sample of 99.99% pure nickel of known saturation magnetic moment. The current was applied to the electromagnet by Agilent power supply up to 8 ampere and the corresponding magnetic field was measured by the Gauss meter. The ratio transformer reading was recorded and magnetization of the samples were calculated using the following equation,

$$M = \frac{KV}{m} \quad \text{emu/g} \quad (1)$$

where, M = Magnetization  
m = Mass of the experimental sample  
V = Voltage correspond to the magnetization  
K = Calibration constant of the VSM

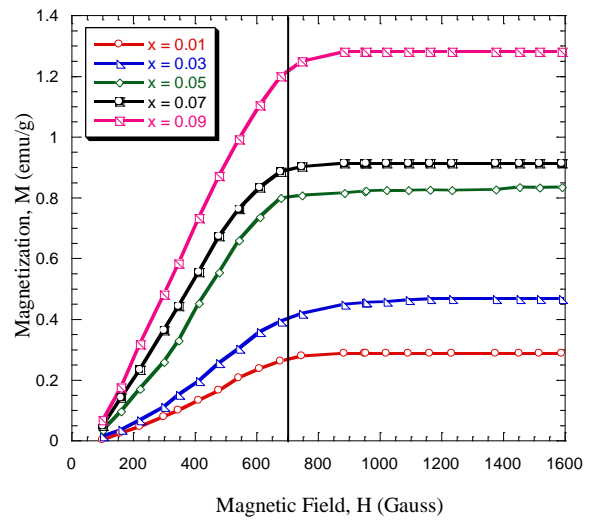


Fig.10: Variation of magnetization with doping of Mn into ZnO at different magnetic field

The magnetization of the samples varies almost linearly up to applied magnetic field of 700 Gauss, after which a saturation magnetization is observed for all samples, as shown in Fig. 10. It is also found that the magnetization is increased as the doping concentration is increased in the samples, which is obvious because magnesium ions are increased with increasing doping concentration in the samples.

#### 4. CONCLUSIONS

In the present work,  $Zn_{1-x}Mn_xO$  ( $x = 0 \leq x \leq 0.09$ ) samples were prepared by solid state reaction method and their structural, electrical, dielectric and magnetic properties were investigated. Based on the experimental results, the following conclusions can be made:

(1) From the XRD analysis, it is clear that there exists only hexagonal ZnO phase in the samples up to  $x \leq 0.05$ . For  $x \geq 0.07$ , there exists both hexagonal ZnO and tetragonal  $MnO_2$  and monoclinic  $Mn_5O_8$  phases.

(2) From the resistance measurement, it is clear that the resistance of the samples increases with the increase of Mn content into ZnO. It is notable that high temperature activation energy varies slightly for Mn/Zn ratio.

(3) Dielectric constant of the prepared samples decreases with increasing frequency and remains almost constant after  $\approx 20$  KHz but depends on Mn/Zn ratio.

(4) Magnetization increased with increasing doping concentration and a saturation magnetization is observed at applied magnetic field of 700 Gauss.

#### 5. ACKNOWLEDGEMENT

The authors acknowledged the Department of Electrical and Electronic Engineering, Toyohashi University of Technology, Japan, for providing XRD facility. The authors are grateful to the Central Science Laboratory, University of Rajshahi, Rajshahi, Bangladesh and also to the Materials science division, Atomic Energy Commission, Dhaka, Bangladesh for providing laboratory facilities.

#### 6. REFERENCES

- [1] R. Viswanatha, S. Sapra, S. S. Gupta, B. Satpati, P. V. Satyam, B. N. Dev and D. D. Sarma, "Synthesis and Characterization of Mn-Doped ZnO Nanocrystals", *Journal of Physical Chemistry B*, vol. 108, pp. 6303-6310, 2004.
- [2] Y. Abdollahi, A. H. Abdullah, Z. Zainal and N. A. Yusof, "Synthesis and characterization of Manganese doped ZnO nanoparticles", *International Journal of Basic & Applied Sciences*, Vol. 11, No. 04, pp. 62-69, 2011.
- [3] A. S. Menon, N. Kalarikkal and S. Thomas, "Studies on structural and optical properties of ZnO and Mn-doped ZnO nanopowders", *Indian Journal of NanoScience*, Vol. 1, pp. 16-24, 2013.
- [4] N. F. Djaja and R. Saleh, "Composition Dependence of Structure and Magnetic Properties in Manganese Doped Nanocrystalline ZnO Particles Prepared by Co-Precipitation", *Materials Sciences and Applications*, Vol. 3, pp. 245-252, 2012.
- [5] R. D. Shannon, "Revised effective ionic radii and systematic studies of interatomic distances in halides and chalcogenides", *Acta Crystallographica*, Vol. 32, pp. 751-767, 1976.

#### 7. NOMENCLATURE

Symbol	Meaning	Unit
$T$	Temperature	(K)
$R$	Resistance	( $\Omega$ )
$E$	Activation energy	(eV)
$M$	Magnetization	(emu/g)
$H$	Magnetic Field	(Gauss)